Optica Applicata, Vol. XLIV, No. 1, 2014
DOI: 10.5277/oa140111

Analysis of the arm spacing effect on symmetric and asymmetric Y-shape optical power splitters: plasmonic interactions between gold nanorings

ARASH AHMADIVAND

Department of Electrical Engineering, Ahar Branch, Islamic Azad University, Ahar, Iran

*Corresponding author: a_ahmadivand@iau-ahar.ac.ir

In this paper, we investigated specific properties and features of several kinds of Y-splitters based on gold nanorings arrays which are surrounded by SiO_2 host substance, to be used at C-band spectrum ($\lambda \sim 1550$ nm). The comparison between two kinds of splitters shows that the symmetric splitter demonstrates better performance than the asymmetric splitter at given wavelength with high efficiency and transmittance (power ratio). Calculations proved that the transmitted power percentage was approximately ~47.5% in the well-organized splitter. It is shown that the offset distance plays an important role in the quality of the optical energy division and transmission through the plasmonic waveguide. The influence of increasing and decreasing in the offset distance was demonstrated numerically by snapshots. Hence, choosing and determining the appropriate value for the offset distance lead to the structure with lower losses and higher percentage in energy transmission. Ultimately, the optical behavior of an asymmetric nanostructure with unequal distances between the arms and the main array is investigated and its applications and possible purposes are introduced.

Keywords: plasmonics, symmetric and asymmetric, splitter and Y-structure, nanoring, offset distance, transmitted power.

1. Introduction

Recently, a remarkable progress and development in designing and producing sub-wavelength and nanoscale photonic structures have been observed [1, 2]. The use of noble metallic nanoparticles which are surrounded by dielectric substance as a host (*e.g.*, SiO_2) in order to transport electromagnetic (EM) waves below the diffraction limit leads to an important aspect of optical physics, namely to a plasmon waveguide. Plasmon waveguides are usually based on nanochains of metal particles that have been used extensively in order to transmit the EM waves at diverse wavelength spectra [3, 4]. When an incident light strongly interacts with these nanoparticles, then, this interaction causes coherent fluctuations of the conduction band free electrons of a nanoparticle. Therefore, these collective electron motions take place at the specific frequency, and are termed the surface plasmons (SPs) and the pertinent frequency is the surface plas-

mon frequency [1–3]. The excitation frequency is in the visible and near-infrared (NIR) region of the spectrum in most of noble metals (*e.g.*, gold, silver, copper *etc.*) [4, 5]. Free electrons oscillations of a nanosized structure that are in the resonance regime with the incident EM wave control the optical properties of the arrangement and this enhancement and localization of the field is known as localized surface plasmon resonance (LSPR). Providing the peak of LSPR at a desired wavelength strongly depends on the structural, physical, and chemical features of the arrangement, it plays an important role in adjusting the maximum amplitude of the optical response at demanded spectra [6, 7].

The resonance frequency of a particular nanoparticle can be determined by shape, geometrical sizes, and chemical characteristics of the employed particles and host material such as a dielectric constant [6]. In simple configurations, the plasmon resonance frequency occurs in the visible spectra for a variety of dielectric substances [7]. Employing the quasi-static approximation in most of former works proved that to provide plasmon resonance near $\lambda \sim 1550$ nm, any shape of metal nanoparticles (nanosphere, nanorods, nanodisks) must be surrounded by a substrate with relative permittivity more than 55, which is not applicable in photonic nanostructures and apparatuses [7, 8]. Hence, to red-shift the LSPR to higher wavelengths, more complex configurations of nanoparticles with an extra degree of freedom (DoF) in geometrical dimensions were demanded, which helped to provide the peak of plasmon resonance at a desired position by making various alterations in their dimensional sizes. Thus, nanoparticles with more than one or two variable dimensional factors are needed and the nanoring is one of the appropriate choices in this case. In comparison to sphere and disk particles, the nanoring permits to obtain a higher decrease in size and flexible tunability because of their exclusive geometrical advantages [7]. Nanoring structural parameters are the radial thickness (t), the inner (R_i) and outer (R) radius, and the height (h), which are used in adjusting the LSPR at the preferred wavelength such as $\lambda \sim 1550$ nm [7]. Transportation of EM field through the plasmonic waveguides via particle arrays is connected with some limitations that must be resolved. Guiding the light below the diffraction limit is one of these restrictions that refer to dimensional and shape limitations of the considered nanostructure [5]. Normal guiding geometry is the other limitation, which shows that examined waveguides are restricted in their geometry due to radiation which escapes at sharp bends and corners [5]. Utilizing the Mie theory and other associated models, the comparison between particle geometrical dimensions and incident wavelength spectrum leads to another important limitation in this concept. If the dimension of a nanoparticle is much smaller than the wavelength of the incident and interacted light ($d \ll \lambda$ – near-field state), then dipoles and higher orders of poles are produced in metal [8, 9]. Considering an array that includes similar nanoparticles that are deposited close to each other, launching an electric field to the first particle causes the excitation of SPs inside the first metal particle and these excitations will be coupled to the neighbor particle due to the near-field coupling effect. During the in-

duction of poles, dipoles are dominant and the influence of higher order poles is negligible due to the near-field coupling nature [6–10]. One of the optical structures that has a wide-range use is a Y-shape EM wave divider (splitter) based on sub-wavelength plasmonic based configurations. Recently, there has been a broad research on the Y-splitters properties and operation qualities [11–13]. These works also proved that the light can be divided into two fields with the same polarization and approximately similar power. AHMADIVAND *et al*. [12] employed Au rings with specific dimensions to design plasmonic splitters which are able to function at telecommunication spectra. Accordingly, there is a number of factors which influenced the performance of the device, and to provide an efficient structure, associated structural parameters must be tuned and adjusted accurately. Offset distance (arm spacing), the major parameter which indicated the space between two arms (branches of a splitter), must be modified correctly to increase the ratio of energy transmission and to minimize the losses ratios [13].

In this paper we have investigated several kinds of Y-splitters, employed in transport which divide the EM energy via employed nanorings along the ordered arrays of nanoparticles. Then, we proposed two main types of Y-splitters (symmetric and asymmetric) and we have studied their features in order to evaluate them. Moreover, the effect of bend degrees and offset distances in transmission efficiency and transmitted power were analyzed to propose a Y-splitter plasmon waveguide with high efficiency. Recent researches have shown that variations in the offset distance between two arms of the Y-splitter have an influence on transmission efficiency, therefore the structure with smaller offset distance demonstrates better performance in optical energy transportation [13, 14]. On the other hand, bigger reduction in the size of this parameter has a destructive effect on the divided fields, and the crucial impact is the interferencing of fields with each other. Therefore, finding an appropriate size for this parameter helps to provide an accurate device with remarkably lower losses. Finite-difference time-domain (FDTD) method has been employed to extract the properties of the proposed and examined devices, and the results of simulations information for each structure will be discussed further. In order to analyze the waveguide features, we used FDTD method for our simulations, because of its appropriate results for modeling plasmon resonance and optical energy transport via an ordered array of nanoparticles due to its geometrical flexibility and matrix-free nature (obviously modernized) [15]. FDTD method has been already employed in modeling and analyzing various shapes and configurations which are associated with the plasmon waveguides.

This paper is organized as follows: in Section 2, by using ordered arrays of Au nanorings in SiO_2 substrate, we have compared various symmetric Y-splitters with different angles and offset distances, and also the best structure with high efficiency and lower losses is selected. In Section 3, the properties and performance of asymmetric Y-splitters are studied. Finally, comparing symmetric and asymmetric Y-splitters leads to choosing the best structure with desired properties (high efficiency and lower losses). Also, specific applications of each examined structure are discussed.

2. Symmetric Y-splitter plasmon waveguides properties

In this section, symmetric Y-shape splitters based on arrays of Au nanorings are examined based on physical and structural dimensions alterations. The spatial distances of each branch to the center axis of the splitter or main entrance array are exactly the same in symmetric structures. As we mentioned in the previous section, in order to transport the EM energy at the optical telecommunication band, we have to find best geometrical sizes for nanorings, their intercenter distance. According to [7], considering an alone Au nanoring in an SiO_2 host with typical refractive index of 1.46 and launching a Gaussian electric field which is placed 330 nm away from the first nanoring, help us to obtain and adjust the red-shift of LSPR around $\lambda \sim 1550$ nm [16]. According to the exclusive characteristics of the nanoring, to provide LSPR at given wavelength, by changing the dimensions and considering the simulation results, the appropriate sizes for our nanoring are listed in Table 1. On the other hand, there are two kinds of gold substances, from the point of view of chemical features which determine the plasmon frequency of the particle. Gold with Johnson–Christy and Palik constants can be considered for employed nanorings. Evaluation of the refractive indices for these two kinds of Au nanoparticles reveals that gold with Palik properties has considerably bigger imaginary part of the refractive index at the desired spectrum, but this value for Johnson–Christy gold is lower and this feature leads to lower absorption of optical power by nanoparticles during the excitation of SPs. Also, gold with Johnson–Christy constants is selected, because FDTD model of the structure must follow the material data [17, 18].

To study the quality and intensity of EM energy transportation via nanorings through the waveguide, non-collective modes must be excited of the wave number $k \neq 0$ [19, 20]. To rise these modes (non-collective modes), we launched a Gaussian electric field which is placed 330 nm away from the first nanoparticle along x-axis (propagation direction). Gaussian electric field operates at an actual bandwidth in the range of 1545–1565 nm. Now, we analyze the effect of structural parameters on the light propagation and division. As we have mentioned already, the offset distance has an important impact on the quality of operating of light along the waveguide. Earlier works show the operation performance of the proposed splitter and also the importance of the offset distance parameter [13]. Here, we study the effect of variations

T a b l e 1. Four final geometrical parameters sizes of an Au nanoring in an SiO_2 substrate, to use at $\lambda = 1550$ nm.

Description	Parameter	Size
Inner radius	R_i	87.5 nm
Total radius	R	123 nm
Thickness	t	35.5 nm
Height	H	35 nm

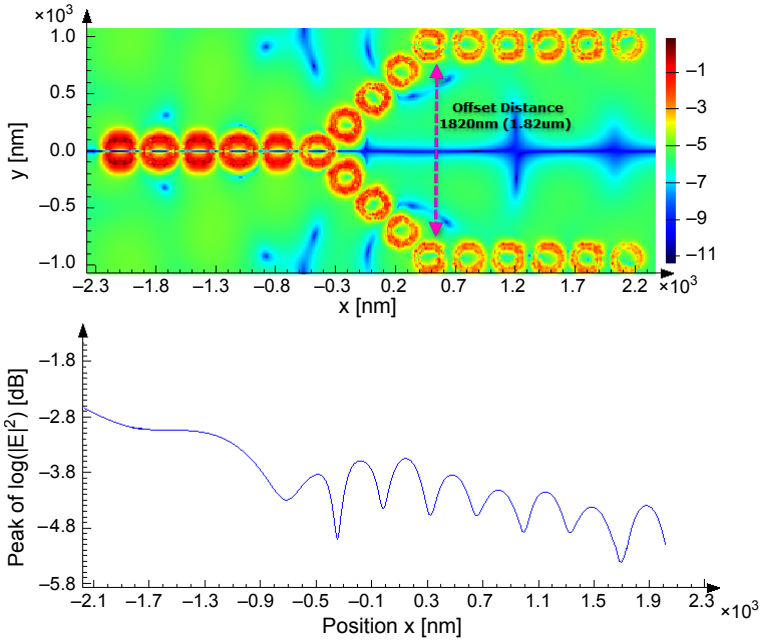

Fig. 1. A snapshot of *xy* view of the symmetric Y-splitter with 45° bend and the offset distance 1.82 μm. This figure shows the field guiding along the chain via Au nanorings. The logarithm of the peak amplitude squared of the electric field along the waveguide is illustrated. This diagram is used for transmission loss calculations.

in this parameter thoroughly. First, we setup the offset distance as d_{offset} = 1.82 μm for the symmetric splitter with the 45° angles degree between each arm and the straight main nanochain. Considering Fig. 1, we are able to probe the splitter properties. This depiction includes a two-dimensional diagram which can be used to calculate the transmission loss factor along the structure, and corresponds to the logarithm of the peak amplitude squared of the Gaussian electric field along the plasmon waveguide. The coupling and resonance intensity of the guided EM wave along the structure decays exponentially:

$$|E|^2 \propto \exp(-\gamma x) \tag{1}$$

where, γ is the loss factor and x is the propagation direction. In this splitter, the loss factor is obtained as 3 dB/455 nm. Transmitted power (power ratio) along the structure and at the output spots of each branch should be computed numerically. In this regime, the real time-averaged power variations along the propagation direction (x-axis) and also the complex Poynting vector relation are applied numerically. Figure 2 demonstrates variations in optical power after the splitting section through the branches in y-axis which use power ratio calculations according to procedures below. Complex

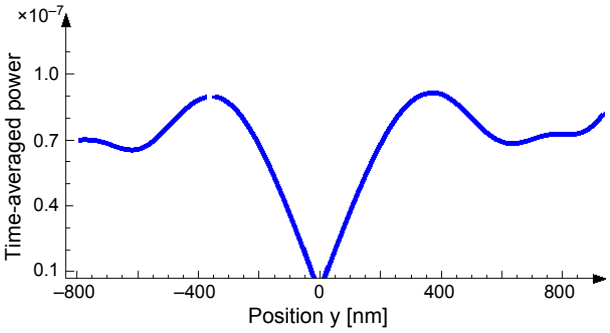

Fig. 2. Real time-averaged power variations after the splitting section in the *y*-axis direction, used in power ratio calculations; the power ratio at each branch is almost 39%.

Poynting vector as $\mathbf{P} = \mathbf{E}(\omega) \times \mathbf{H}^*(\omega)$ must be taken into account during the series of calculations.

The guided power is related to the real part of the complex Poynting vector. The factor of 1/2 indicates the time averaging of the clockwise (CW) fields. The imaginary part of the Poynting vector relates to the non-propagating reactive or stored optical energy (which is not related to our computations). Considering the real time-averaged power variations along the *y*-axis for monitored and incident optical energies, we are able to present the transmitted power as below [12, 13]:

$$T(\omega) = \frac{\frac{1}{2}\int \mathrm{Real}\left[P_y^{\mathrm{Monitor}}(\omega)\right]\mathrm{d}x}{\frac{1}{2}\int \mathrm{Real}\left[P_x^{\mathrm{Source}}(\omega)\right]\mathrm{d}x} \tag{2}$$

Accordingly, the monitored power for this structure is calculated as approximately 39% at each branch and the missing part of the field is scattered and absorbed by nanochains particles and some is dissipated by inherent lossy waveguide. But, this low percentage of power is associated with the lossy behavior of plasmon waveguides and the offset distance as well. Plasmon waveguides are natively lossy which is the reason for emerging of various losses while transporting energy. In order to increase the power ratio in a proposed splitter and reduce the impact of losses, we alter the size of the offset distance. For the first step, we decrease the offset distance from 1.82 to 1.32 μm. The angle's degree between each arm and the straight main array is 30°. The logarithmic scale of field intensity along the propagation direction and simulation results are illustrated in Fig. 3. Accordingly, the transmission loss factor for this structure is calculated as 3 dB/545 nm. The inset snapshot demonstrates the excitation of SPs inside the nanorings and their coupling, transporting, and dividing performances in a two-dimensional image. Also, the real time-averaged power variation along the *x*-axis is de-

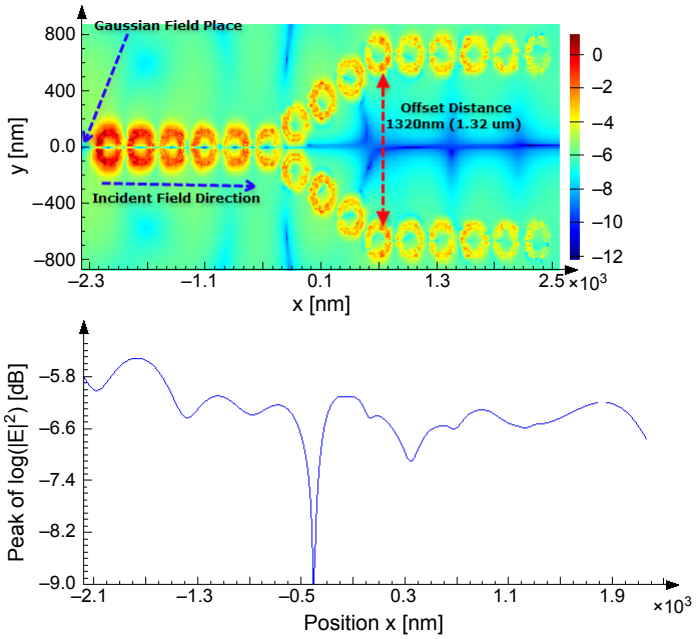

Fig. 3. The logarithm of the peak amplitude squared of the electric field along the waveguide is illustrated. This diagram is used for transmission loss calculations. The inset snapshot is a *xy* view of the symmetric Y-splitter with 30° bend and the offset distance is 1.32 µm. This figure shows the field guiding along the chain via Au nanorings.

picted in Fig. 4. Considering the mentioned equations and this figure, we are capable of computing the power ratio for this structure as ~47.5%. Consequently, this structure shows better performance in comparison to the former structure. More reduction in offset distance will be feasible but the interference of divided fields at each branch cannot be estimated due to the intensity of coupling dipoles.

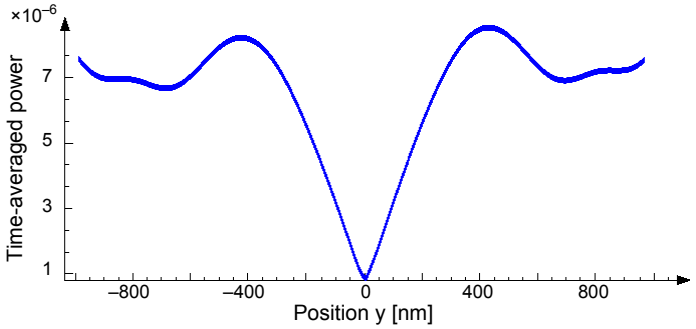

Fig. 4. Real time-averaged power variations after the splitting section in the *y*-axis direction, used in power ratio calculations; the power ratio at each branch is almost 47.5%.

3. Asymmetric Y-splitter plasmon waveguides properties

In this section, we examine the effect of an asymmetric regime in an Y-splitter with strange and different arm spacing (offset distance). Asymmetric structures, such as polarization beam splitters and tunable power splitters [21–23], and couplers [24, 25], have a wide range of use in designing optical nanosized structures. By setting one of the splitter arms at 30° angle and another arm angle with a straight chain set to 45°, the offset distance is set to 1.6 μm. Now, we have an asymmetric Y-splitter based on arrays of Au nanorings. The logarithmic scale of the peak of field intensity is illustrated in Fig. 5. In addition, this figure contains a two-dimensional snapshot of energy guiding along the waveguide. A significant reduction in a propagating pulse can be noticed. Accordingly, the transmission loss factor is calculated as 3 dB/622 nm. On the other hand, to determine the percentage amount of transmitted power, Fig. 6 (real time-averaged power variation *versus* the *x*-axis) and related equations must be taken into account. Accordingly, the power ratio is almost 41.5% at the branch with 30° angle and for the 45° branch it is ~36.5%. Ultimately, it is clear that the asymmetry of Y-splitter due to its lower efficiency in power transmission and higher losses cannot be an appropriate choice in regular integrated photonic devices and it has some specific appli-

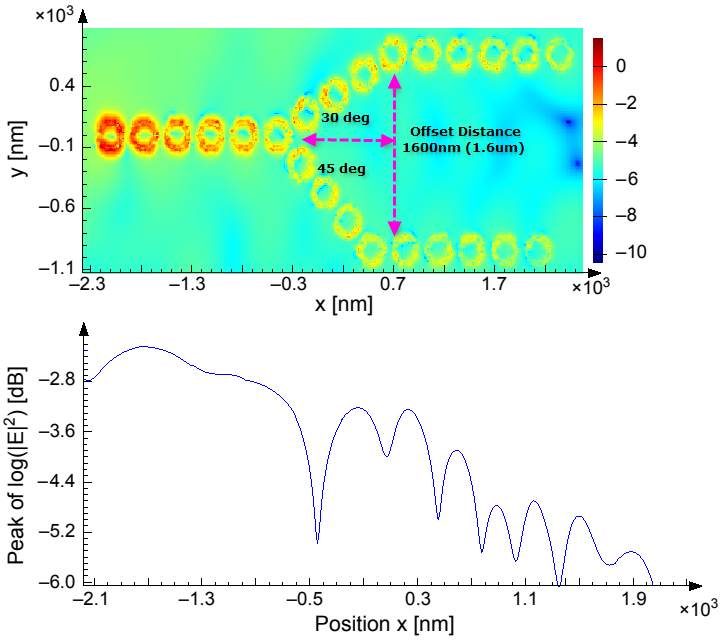

Fig. 5. A snapshot of a *xy* view of the asymmetric Y-splitter with blend of 30° and 45° bends and the offset distance 1.6 μm. This figure shows the field guiding along the chain via Au nanorings. The logarithm of the peak amplitude squared of the electric field along the waveguide is illustrated. This diagram is used for transmission loss calculations.

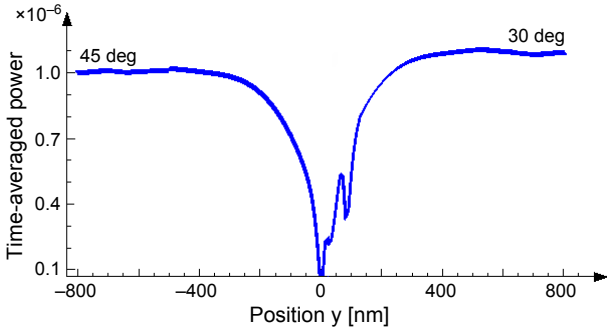

Fig. 6. Real time-averaged power variations after the splitting section in the *y*-axis direction, used in power ratio calculations; the power ratio at each branch is almost 41.5%.

T a b l e 2. FDTD model simulation parameters, sizes, and descriptions.

FDTD parameter description	Quantities/Situation
Cell numbers	7500
Spatial cell size ($d_x = d_y = d_z$)	5 nm
Number of time step	9000
Number of snapshots	11340
Simulation time	2000 fs
Background index	1
Boundary conditions (PML)	12 layers

cations in beam splitters or couplers in which the acute symmetry of light is not important. All of the simulation parameters in FDTD model such as spatial cell sizes, number of snapshots, and number of time steps, *etc*., are listed in Table 2. Furthermore, boundary conditions as an important factor in FDTD model are considered as perfectly matched layers (PML) with 12 layers to absorb the scattered fields and to prevent their interference in guided EM waves.

4. Conclusions

In this paper we employed the deposited Au nanoring chains in an SiO_2 substance to devise and present various kinds of Y-splitters plasmon waveguides, in order to transport and split the EM energy in nanoscale optical devices at an optical communication band ($\lambda \sim 1550$ nm). In this paper, symmetric Y-splitters based on nanoring chains with 30° and 45° bends and with corresponding offset distances as 1.32 and 1.82 μm have been analyzed, respectively. Our studies demonstrated that the transmitted power in these two splitters is approximately 39% and 47.5% for bigger and shorter arm spacing, respectively. Finally, the properties of an asymmetric Y-splitter plasmon waveguide

with 1.6 μm offset distance have been analyzed, and simulation results showed that this structure has lower efficiency in comparison to the symmetric nanostructures; the corresponding power ratio percentage is ~41.5%. In spite of some associated problems, the asymmetric configuration has specific applications and is widely used in polarization beam splitters or certain couplers.

References

[1] KREIBIG U., VOLLMER M., *Optical Properties of Metal Clusters*, Springer-Verlag, Berlin, 1995.

[2] RAETHER H., *Surface Plasmon on Smooth and Rough Surface and Grating*, Springer-Verlag, Berlin, 1986.

[3] MAIER S.A., *Plasmonics: Fundamentals and Applications*, Springer, 2007.

[4] BRONGERSMA M.L., HARTMAN J.W., ATWATER H.A., *Electromagnetic energy transfer and switching in nanoparticle chain arrays below the diffraction limit*, Physical Review B **62**(24), 2000, pp. R16356–R16359.

[5] SALEH B.E.A., TEICH M.C., *Fundamentals of Photonics*, Wiley, New York, 1991.

[6] MAIER S.A., BRONGERSMA M.L., KIK P.G., MELTZER S., REQUICHA A.A.G., ATWATER H.A., *Plasmonics – A route to nanoscale optical devices*, Advanced Materials **13**(19), 2001, pp. 1501–1505.

[7] KYUNG-YOUNG JUNG, TEIXEIRA F.L., REANO R.M., *Au/SiO_2 nanoring plasmon waveguides at optical communication band*, Journal of Lightwave Technology **25**(9), 2007, pp. 2757–2765.

[8] BOHREN C.F., HUFFMAN D.R., *Absorption and Scattering of Light by Small Particles*, Wiley, New York, 1983.

[9] JACKSON J.D., *Classical Electrodynamics*, 3rd Ed., Wiley, 1998.

[10] AHMADIVAND A., GOLMOHAMMADI S., ROSTAMI A., *Broad comparison between Au nanospheres, nanorods, and nanorings as an S-bend plasmon waveguide at optical C-band spectrum*, Journal of Optical Technology **80**(2), 2013, pp. 80–87.

[11] AHMADIVAND A., *Enhancement of L-junction plasmon waveguides properties using various shapes of nanoparticles arrays at $\lambda \approx 1550$ nm*, Advances in Digital Multimedia **1**(1), 2012, pp. 1–3.

[12] AHMADIVAND A., GOLMOHAMMADI S., ROSTAMI A., *T- and Y-splitters based on an Au/SiO_2 nanoring chain at an optical communication band*, Applied Optics **51**(15), 2012, pp. 2784–2793.

[13] AHMADIVAND A., GOLMOHAMMADI S., *Comprehensive investigation of noble metal nanoparticles shape, size, and material on the optical response of optimal plasmonic Y-shape waveguides*, Optics Communications **310**, 2014, pp. 1–11.

[14] AHMADIVAND A., *Routing properties of the T-structure based on Au/SiO_2 nanorings in optical nanophotonic devices*, Optica Applicata **42**(3), 2012, pp. 659–666.

[15] TAFLOVE A., HAGNESS S.C., *Computational Electrodynamics: The Finite-Difference Time-Domain Method*, 2nd Ed., Artech House, Norwood, MA, 2000.

[16] RAYFORD C.E., SCHATZ G., SHUFORD K., *Optical properties of gold nanospheres*, Nanoscape **2**(1), 2005, pp. 27–33.

[17] MOCK J.J., SMITH D.R., SCHULTZ S., *Local refractive index dependence of plasmon resonance spectra from individual nanoparticles*, Nano Letters **3**(4), 2003, pp. 485–491.

[18] PALIK E.D., *Handbook of Optical Constants of Solids*, Academic Press, 1991.

[19] MAIER S.A., KIK P.G., ATWATER H.A., *Optical pulse propagation in metal nanoparticle chain waveguides*, Physical Review B **67**(20), 2003, article 205402.

[20] HOLMGAARD T., ZHUO CHEN, BOZHEVOLNYI S.I., MARKEY L., DEREUX A., KRASAVIN A.V., ZAYATS A.V., *Bend- and splitting loss of dielectric-loaded surface plasmon-polariton waveguides*, Optics Express **16**(18), 2008, pp. 13585–13592.

[21] AHMADIVAND A., *Hybrid photonic–plasmonic polarization beam splitter (HPPPBS) based on metal–silica–silicon interactions*, Optics and Laser Technology **58**, 2014, pp. 145–150.
[22] LEUTHOLD J., JOYNER C.H., *Multimode interference couplers with tunable power splitting ratios*, Journal of Lightwave Technology **19**(5), 2001, pp. 700–707.
[23] HAYAKAWA T., ASAKAWA S., KOKUBUN Y., *Arrow-B type polarization splitter with asymmetric Y-branch fabricated by a self-alignment process*, Journal of Lightwave Technology **15**(7), 1997, pp. 1165–1170.
[24] ALMEIDA V.R., QIANFAN XU, BARRIOS C.A., LIPSON M., *Guiding and confining light in void nanostructure*, Optics Letters **29**(11), 2004, pp. 1209–1211.
[25] EHSAN A.A., SHAARI S., *Assymetric Y-branch plastic optical fiber coupler*, Optica Applicata **41**(4), 2011, pp. 807–816.

Received September 3, 2013
in revised form December 26, 2013